

## Antenna Technologies for 5G and Beyond Wireless Communications

Marwan Krunz  
 ED2 Chief Scientist representing partner Wilson Electronics

### Introduction

The wireless industry has been racing to bring to market efficient Fifth Generation (5G) solutions in support of three main use cases: Enhanced mobile broadband (eMBB), ultra-reliable low-latency communications (URLLC), and massive machine-type communications (mMTC). By now, it has become clear that

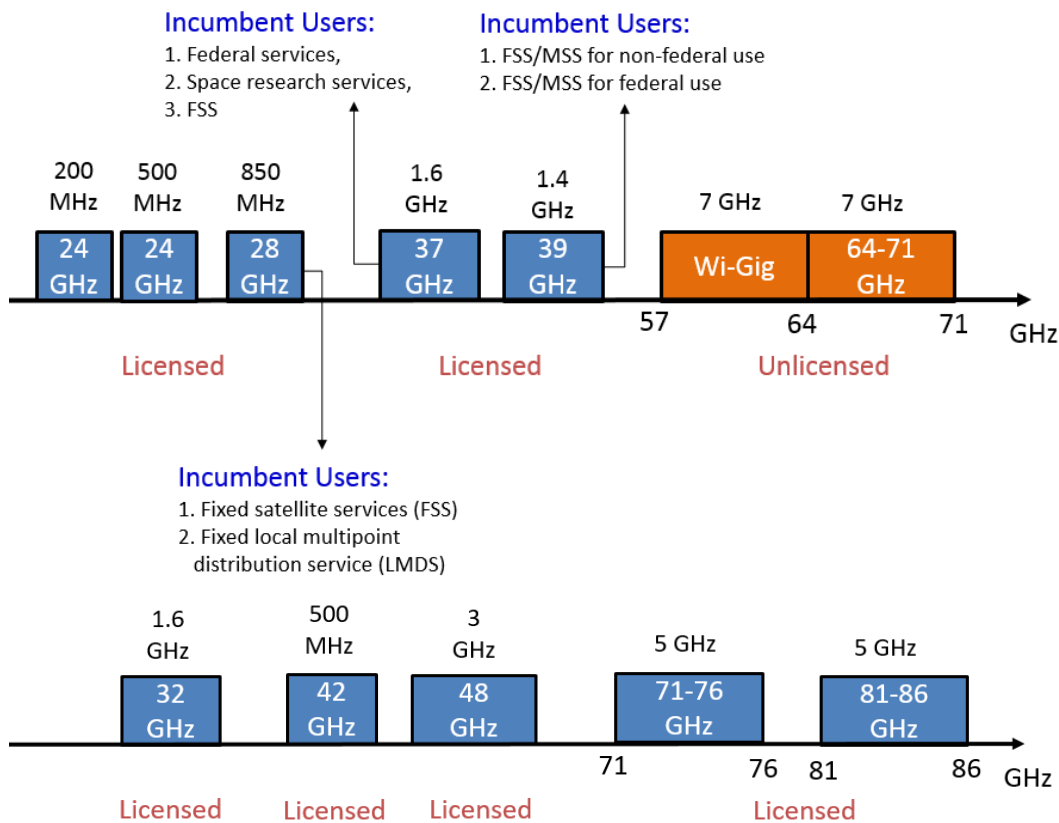


Figure 1: mmWave spectrum for broadband wireless: (a) current allocation in the US (licensed and unlicensed); (b) some of the bands under consideration by the FCC. Part (a) also shows legacy incumbents of some mmWave bands.

transitioning from the existing LTE technology (the most common form of 4G) to 5G is by no means incremental, especially for 5G systems that operate in the millimeter-wave (mmWave)

spectrum. According to the 3GPP specifications, 5G mmWave spectrum, officially known as Frequency Range 2 (FR2), includes several bands that start from 24.25 GHz and go all the way to 52.6 GHz, with higher frequencies up to 95 GHz and beyond under study. Not all 3GPP FR2 bands are available in every region in the world. For instance, US operators have primarily focused on the 24 GHz (24.25-24.45 GHz and 24.75-25.25 GHz), 28 GHz (27.5-28.35 GHz), Upper 37 GHz (37.6-38.6 GHz), 39 GHz (38.6-40 GHz), and 48 GHz (47.2-48.2 GHz) bands. Recently, with the intent to open more spectrum for use in 5G, Internet of Things, and other advanced spectrum-based services, the FCC proposed new rules for the 42-42.5 GHz and 50.4-52.6 GHz bands. It also sought comments on applying these rules to the 26 GHz band (25.25-27.5 GHz).

Despite their impressive capacity, mmWave frequencies suffer from high signal attenuation loss, poor penetration of walls/objects (hence, blockage issues), and limited scattering. Specifically, the path loss of an electromagnetic wave scales inversely with the square of its frequency. Thus, a signal transmitted at, say, 30 GHz will experience 100 times (20 dB) more attenuation than a signal transmitted at 3 GHz, assuming the same transmit power and channel bandwidth. Penetration losses at mmWave frequencies are also significant, often exceeding 35 dB for bricks and concrete. Even the human body is known to cause serious blockage to mmWave transmissions. Such issues make it particularly challenging to support *uniform* 5G services, especially under user mobility.

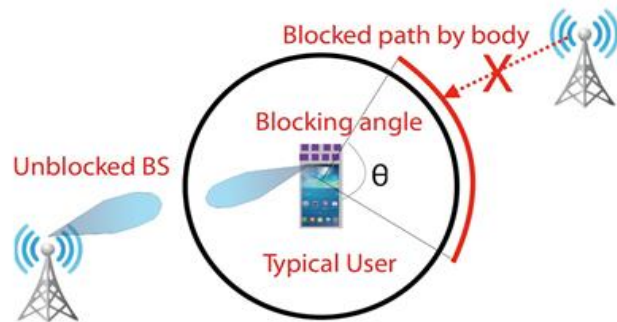


Figure 2: Blockage problems at mmWave frequencies.

At the same time, the small wavelengths of mmWave bands allow many antenna elements to be packed onto a small-form-factor device. With proper processing of the signals fed into these antennas, transmissions can be beamed along a desired direction. This way, the severe signal attenuation over mmWave bands can be compensated for by the resulting beamforming gain. Besides the increased gain, beam directionality allows for a significant boost in the spatial reuse, whereby multiple spatially separated users can be served by the same base station (BS) at the same time and over the same frequency (see Figure 3).

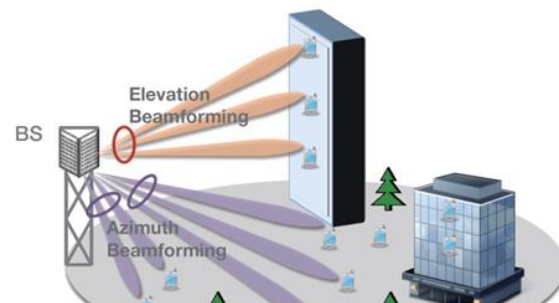


Figure 3: Increasing the spatial reuse of cellular systems using narrow beams.

Different antenna technologies have been advocated for mmWave operation in 5G

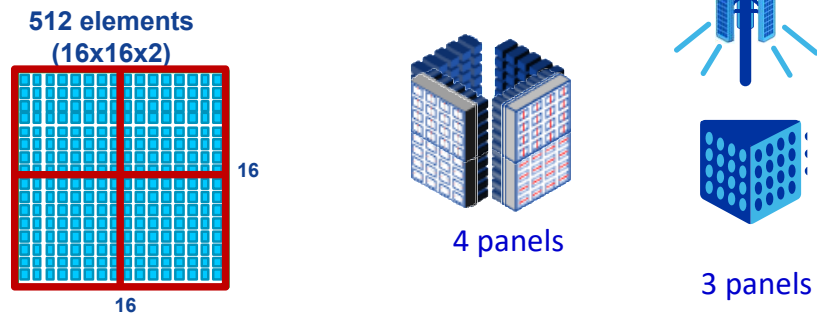
systems. These include: (1) electronically steerable arrays, (2) dielectric waveguide antennas, and (3) lens-based arrays. These designs offer the ability to produce multiple analog beams, but they differ in the underlying technology, beamforming capability, power consumption, and others. In the rest of this article, we focus on the first two technologies and explain their salient features. For brevity, we restrict the treatment to analog beamforming architectures, noting that both technologies can be augmented with digital beamforming, thereby enabling hybrid beamforming designs.

## Antenna Technologies

### Electronically Steerable Antenna Arrays

Electronically steerable antenna arrays have been widely used in 5G products, owing to their well-understood characteristics and the ability to integrate them with RFICs. In its simplest form,

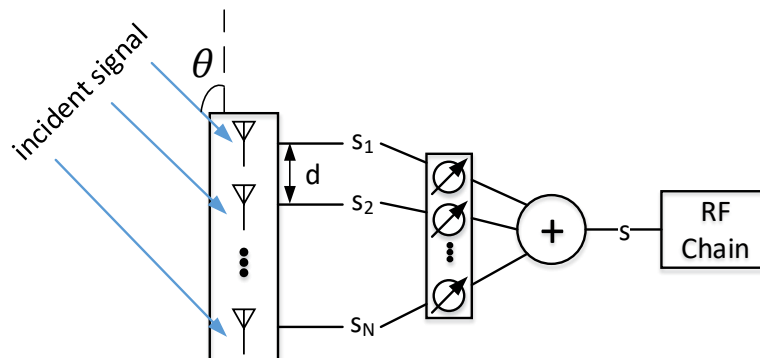
an electronically steerable array is comprised of one or more “panels”, each containing a rectangular grid of antenna elements, typically patch antennas. The antennas are spaced out by  $\lambda/2$  or more, where  $\lambda$  is the carrier wavelength; see Figure 4. A typical patch antenna consists of a



Panel partitioned into 4 subarrays

Figure 4: Examples of electronically steerable antenna arrays: A 16-by-16 dual-polarized array that is partitioned into 4 subarrays (left); multiple partitions based on 4 panels (middle); and a 3-panel partition (right) [source: Nokia Networks].

conductive surface that is separated from a conductive ground plane by a dielectric layer. Its gain is  $\sim 6-8$  dBi (dBi is the gain in dB relative to an isotropic antenna), with an associated half-power beamwidth (HPBW) of about 65 deg. To generate a narrow beam and steer it electronically, complex weights are applied to the various antenna elements in the RF domain. These weights are obtained by calculating the *array factor* (AF). The matrix of



complex weights is implemented using phase shifters.

To illustrate the basic idea behind electronically steerable antennas, we consider a receiver (Rx) that is equipped with a uniform linear array (ULA); see Figure 5. A similar discussion applies to beamforming at the transmitter (Tx). Let  $N$  and  $F_{\text{ULA}}$  denote the number of antennas and the AF for the ULA. The Rx receives a signal from a plane wave at an incident angle  $\theta$ , as shown in the figure. Because the transmission paths are not equal, the received signal has different phase shifts at different antenna elements. For a ULA, adjacent elements are separated by the same distance  $d$ , leading to a linear array of total length  $(N - 1)d$ . Note that the phase of antenna element  $n$  leads the phase of element  $n - 1$  by  $(2\pi d \cos \theta)/\lambda$ . Thus, we can write the received signal at antenna  $n$ ,  $n \in \{1, \dots, N\}$ , as:

$$s_n = R I_n e^{j2\pi n d \cos \theta / \lambda}$$

where  $I_n$  is the amplitude excitation of the  $n$ th element and  $R$  is the radiation pattern of each antenna element (in a uniform array, elements are typically assumed to have the same  $R$ ). Because  $I_n$  does not affect the analog beamforming weights, without loss of generality, we assume  $I_n = 1$ .

Let  $s$  be the overall signal of the antenna array. This  $s$  is a weighted sum of  $s_n$ 's, with each  $s_n$  multiplied by a complex weight  $w_n$ :

$$s = R \sum_{n=1}^N w_n e^{j2\pi n d \cos \theta / \lambda} = R F_{\text{ULA}}$$

Assuming the same signal magnitude at each antenna, the signal power at the antenna array can be maximized by maximizing  $|R F_{\text{ULA}}|$ , or equivalently  $|F_{\text{ULA}}|$ . This  $|F_{\text{ULA}}|$  can be maximized by selecting  $w_n$  in a way to ensure that the received signals are in phase, i.e., by setting  $w_n = e^{-j2\pi n d \cos \theta / \lambda}$ . To achieve that, the phase of the signal received by the  $N$ th antenna is kept the same, and the phase of the signal received by every other antenna element  $n$ ,  $n = 1, \dots, N - 1$ , is shifted by  $(N - n)2\pi d \cos \theta$ .

Next, we extend the treatment to a rectangular uniform planar array (UPA), commonly found in 5G products. Consider a UPA with a horizontal inter-element distance  $d_x$  and a vertical inter-element distance  $d_y$ . In this case, we denote the AF by  $F_{\text{UPA}}$ . Suppose that the incident wave of the received signal arrives at a polar angle  $\theta$  and azimuth angle  $\alpha$ , and that the antennas are placed on an  $M$ -by- $N$  grid, as shown in Figure 4. Following similar analysis to that of the ULA, we can write the received signal at antenna element  $(m, n)$  as:

$$s_{m,n} = R e^{j2 \pi (d_x m \cos \alpha \sin \theta + d_y n \sin \alpha \sin \theta) / \lambda}$$

where  $m \in \{1, \dots, M\}$  and  $n \in \{1, \dots, N\}$ . Likewise, the received signal  $s$  after beamforming with complex phase-shift weights  $w_{m,n}$  can be written as:

$$s = R \sum_{m=1}^M \sum_{n=1}^N w_{m,n} e^{j2 \pi (d_x m \cos \alpha \sin \theta + d_y n \sin \alpha \sin \theta) / \lambda} = R F_{\text{UPA}}$$

The complex weights that maximize the AF are given by:

$$w_{m,n} = e^{-j2 \pi (d_x m \cos \alpha \sin \theta + d_y n \sin \alpha \sin \theta) / \lambda}$$

With such weights, the beam can be steered along the direction  $(\theta, \alpha)$ , as shown in Figure 4(b).

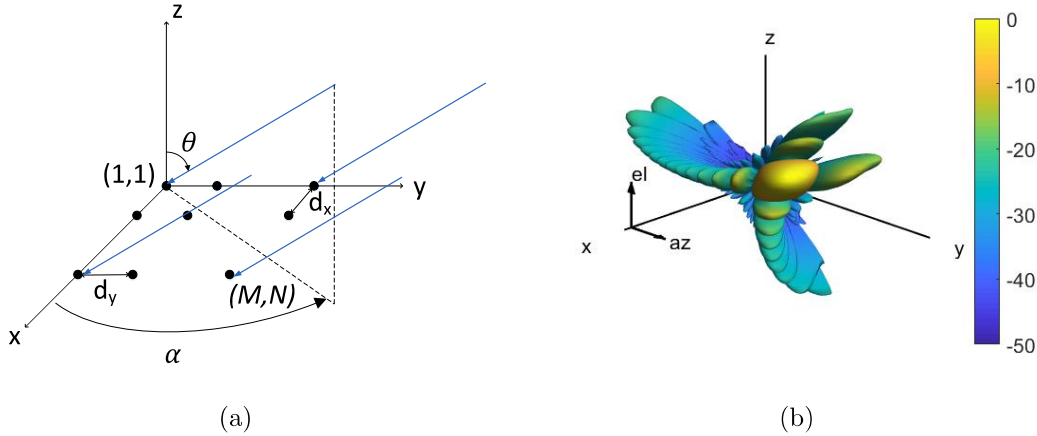


Figure 4: (a) Illustration of analog Rx beamforming using an electronically steerable UPA (angle of desired Rx direction is  $(\theta, \alpha)$ ), (b) normalized 3D directivity pattern of a 16-by-16 UPA, where  $\theta = 45^\circ$  and  $\alpha = 15^\circ$  (UPA placed on the Y-Z plane).

To beamform along a given direction, the channel matrix between a BS and a user equipment (UE) must first be determined. Let the total number of antennas at the BS and the UE be  $A_{\text{BS}} = M_{\text{BS}} N_{\text{BS}}$  and  $A_{\text{UE}} = M_{\text{UE}} N_{\text{UE}}$ , respectively. Here,  $M_i$  and  $N_i$ ,  $i \in \{\text{BS}, \text{UE}\}$ , refer to the number of rows and columns in the UPA. At mmWave frequencies, the channel does not exhibit rich scattering; instead, it exhibits a clustering behavior where the various rays arrive at the Rx along a few angular clusters (2-4 clusters are commonly found at 28 GHz frequency). Consider the  $p$ th

cluster,  $p = 1, \dots, P$ . Let  $\mathbf{a}_B(\theta_p', \alpha_p')$  denote the  $A_{BS} \times 1$  array response vector (ARV) of the BS antenna system and  $\mathbf{a}_U(\theta_p, \alpha_p)$  denote the  $A_{UE} \times 1$  ARV of the UE antenna system for channel cluster  $p$ . ARV consists of the phases of arriving signals at the antenna elements along a certain direction, with the first antenna taken as the baseline. Here,  $(\theta_p, \alpha_p)$  and  $(\theta_p', \alpha_p')$  are the angle-of-arrival (AoA) and angle-of-departure (AoD) for cluster  $p$  at the time of reception or transmission, respectively. Then, the  $A_{UE} \times A_{BS}$  channel matrix  $\mathbf{H}$  between the BS and the UE can be expressed as:

$$\mathbf{H} = \sum_{p=1}^P h_p \mathbf{a}_U(\theta_p, \alpha_p) \mathbf{a}_B^*(\theta_p', \alpha_p')$$

where  $(.)^*$  denotes conjugate transpose operation,  $P$  is the number of clusters, and  $h_p$  is the gain of the  $p$ th cluster (a complex number). An example channel is visualized in Figure 5.

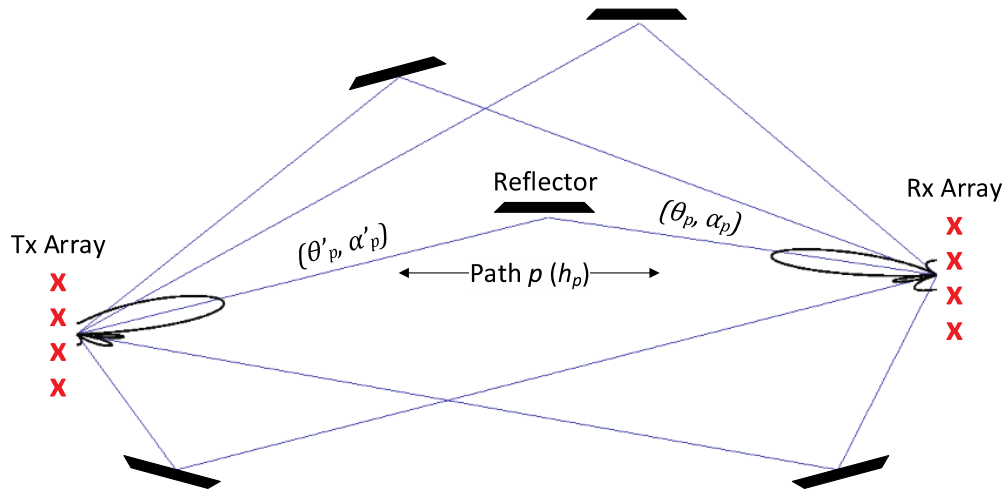


Figure 5: Projection of the representative 3D mmWave channel between a Tx and an Rx array on X-Y plane.

To express the received signal, BS and UE beamforming should be applied to channel  $\mathbf{H}$ . In general, beamforming vectors are computed offline for a set of directions and stored in codebooks at the BS and UE. This codebook-based approach is much faster than designing coherent precoder and combiner vectors on-the-fly based on channel measurements. Let  $Q = \{\mathbf{q}_1, \mathbf{q}_2, \dots, \mathbf{q}_{D_{UE}}\}$  denote the codebook of the UE beamformer and  $F = \{\mathbf{f}_1, \mathbf{f}_2, \dots, \mathbf{f}_{D_{BS}}\}$  denote the codebook of the BS beamformer, where  $D_{UE}$  and  $D_{BS}$  are the maximum numbers of narrow beams that can be generated at the UE and BS, respectively. Both numbers depend on the resolution of the phase shifters of the UPAs. If the BS uses a transmit beamforming vector

$\mathbf{f}_i \in F$  and the UE uses a receive beamforming vector  $\mathbf{q}_j \in Q$ , the received signal  $y_{ij}$  can be expressed as:

$$y_{ij} = \mathbf{q}_j^* \mathbf{H} \mathbf{f}_i x + \mathbf{q}_j^* \mathbf{n}$$

where  $x$  is the transmitted signal and  $\mathbf{n}$  is a matrix whose entries are taken as complex circularly symmetric white noise.

For electronically steerable planar arrays, the beamwidth is dictated by the array size. Theoretically, the half-power beamwidth (HPBW) is given by  $2\left(\frac{\pi}{2} - \cos^{-1}\left(\frac{1.39\lambda}{\pi Nd}\right)\right) \approx 0.886\lambda/(Nd)$ , where  $N$  is the number of antenna elements in a given dimension and  $d$  is the spacing between two adjacent elements. Thus, for a given center wavelength  $\lambda$ , the HPBW is inversely proportional to the antenna aperture ( $Nd$ ). Adjusting the HPBW would therefore require adjusting the size of the antenna array, e.g., for a 16-by-16 array and  $d = 0.5\lambda$ , the HPBW is about  $6.34^\circ$ , the HPBW for a 4-by-4 array is  $25.56^\circ$ .

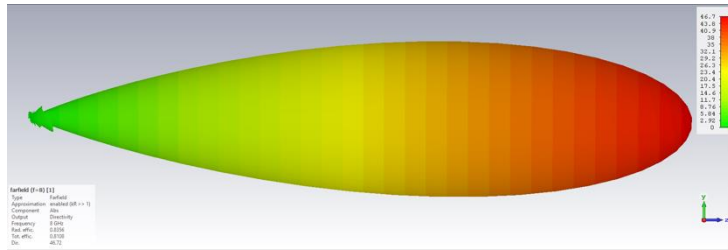
### Dielectric Waveguide Antennas

In contrast to electronically steerable arrays, *dielectric waveguide* antennas (or simply, dielectric rods) do not rely on electronically combining the patterns of an array of antennas. Instead, one dielectric rod acts as a directional antenna, radiating a narrow beam whose HPBW is proportional to the RF frequency and antenna length. The rod itself is made of a special dielectric material. When excited by a conductive element, the rod behaves as an end-fire antenna, producing a beam parallel to the rod's axis. An example of a basic dielectric waveguide antenna is shown in Figure 6. Different shapes may be used (e.g., cylindrical, cone, tapered cone, etc.), with certain impact on the antenna pattern. Figure 7 shows the antenna pattern of a tapered-cylindric rod, designed for the 28 GHz band (the n261 5G NR band).

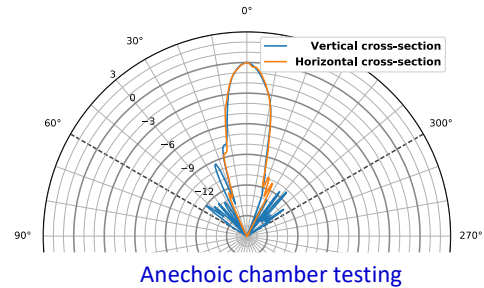


Figure 6: Cylindrically shaped dielectric rod (length = 10 cm, operating freq. = 28 GHz). Approximately 20dBi gain.





Beam shape of a single rod (20° HPBW, CST simulations)



Anechoic chamber testing

Figure 7: Antenna pattern of a tapered-cylindrical dielectric rod of Figure 8. Left figure shows CST simulations; right figure shows Anechoic chamber testing.

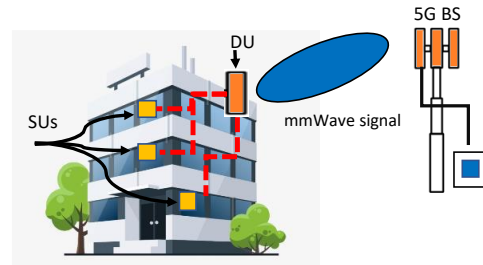
Although the dielectric waveguide concept has been around for a long time, its adaptation for and integration into 5G mmWave products have only been recently pioneered by ED2. In contrast to an electronically steerable array, whose HPBW is adapted by changing the dimensions of the array, the HPBW for a dielectric rod is adapted by changing its length. For example, a cylindrically shaped dielectric rod of electrical length  $L_\lambda$  has a (theoretical) HPBW of  $\frac{60^\circ}{\sqrt{L_\lambda}}$ . To produce, say, a 20° HPBW, one needs a rod of length  $L_\lambda = 9\lambda$ . This corresponds to slightly more than 9 cm at 28 GHz. As 5G/6G systems move to higher mmWave bands, the required rod length is even smaller, e.g., 3.75 to 4.3 cm for frequencies between 70 and 80 GHz. It is possible to adjust the length and geometric properties of the rod to achieve a desired beamwidth at any target mmWave frequency. For example, ED2 has built and tested 28 GHz band dielectric antennas with beamwidths ranging from 90° all the way down to 20°. Depending on rod length (beam widths) gain ranges from 20dBi at the narrowest to approximately 8dBi at the widest. The wide-beam rod is used in the Service Unit (SU) of a 5G mmWave repeater, whereas the narrow-beam antenna is integrated into the donor unit (DU) of the repeater, pointing towards the 5G gNB (see Figure 8). The flexibility of the architecture enables systems to be deployed into a wide variety of use cases.

From a 5G and Beyond (B5G) perspective, the dielectric rod is a disruptive antenna technology that offers significant advantages over state-of-the-art electronically steerable arrays, in both indoor and outdoor scenarios. Specifically, a single rather inexpensive dielectric rod replaces an electronically steerable array/subarray made of tens of patch antennas. With a dielectric rod, no

Figure 8: Example application of the dielectric antenna in indoor 5G mmWave repeaters (DU: Donor Unit, SU: Service Unit).



phase shifters are needed, resulting in significant reduction in cost, power consumption, and silicon area. Note that for a 5G repeater application, dynamic beam steering is unnecessary because the DU needs to be steered only once along the line-of-sight (LOS) direction of a fixed 5G gNB. Such pointing can be done mechanically, as illustrated in the repeater in Figure 9.



For some use cases, multiple dielectric rods may be used to point along different directions. For example, the SU of a 5G mmWave repeater may support two (or more) groups of UEs, which are clustered along two different directions, e.g., North and South of a street intersection where the repeater is deployed. Each cluster is served by one dielectric rod. The two rods may be connected to the same RF chain, with a proper switching mechanism that alternates between the two user groups, or they may be connected to two separate RF chains (functionally, this is equivalent to using two single-direction SUs).

Compared to electronically steerable arrays, dielectric waveguides enjoy more consistent beam characteristics, including symmetric antenna patterns and low side-lobe gain, independent of the UE's location. Specifically, in traditional electronically steerable planar arrays, the HPBW as well as the antenna pattern change when the UE moves away from the broadside of the antenna's ground plane. An example of that is shown in Figure 10 for an 8-by-8 UPA at 28 GHz frequency. When the UE's location is aligned with the broadside of the UPA ( $\theta = 0$ ), the optimal electronically steerable beam has a HPBW of  $12.8^\circ$  and a maximum gain of 22.75 dBi. By rotating the UE by  $\theta = 60^\circ$  while keeping the same distance from the center of the array, the HPBW for the optimal



Figure 9: 5G mmWave repeater that relies on dielectric waveguide antennas (inside the DU/SU boxes).

beam increases to  $28.75^\circ$  and the gain goes down to 19 dB. The antenna pattern also changes, including the intensity and locations of the side lobes. In contrast, in a dielectric antenna, no beam steering is performed, so these effects are not present as long as UEs remain within the HPBW of the dielectric rod.

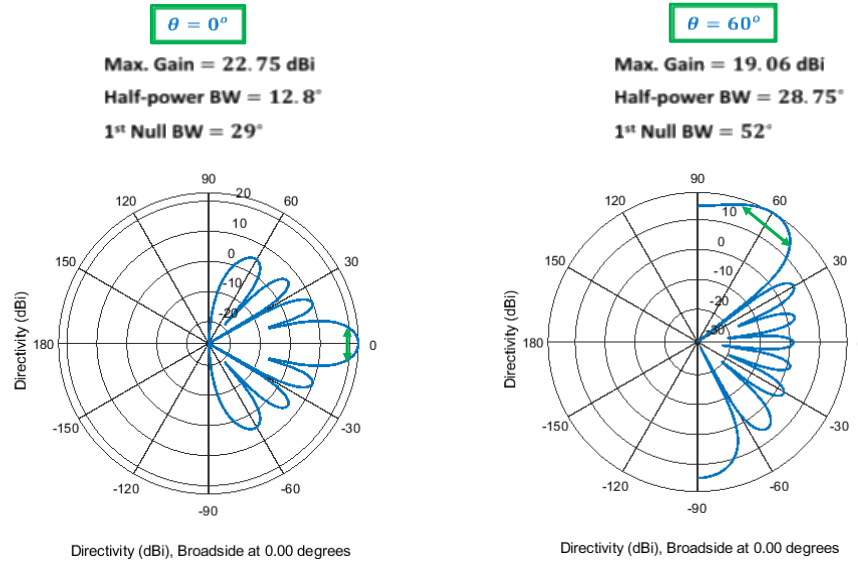


Figure 10: Antenna pattern for an 8-by-8 uniform planar array at 28 GHz. Left figure is when antenna array is electronically beamformed in the direction of the broadside ( $\theta = 0^\circ$ ). Right figure is when array is beamformed  $\theta = 60^\circ$  off the broadside, with a metallic reflector in the back.

Another advantage of the dielectric rod is its wide bandwidth, particularly at mmWave frequencies. Figure 11 depicts the reflection coefficient (S11 parameter) of a dielectric rod that was optimized for the 5G NR n257 band (26.5 to 29.5 GHz). Values below  $-15$  dB are indicative of very low return loss, i.e., most of the power is radiated out of the antenna.

Dielectric rods can also be designed to support various forms of polarization, including linear (V or H), dual-, and circular polarization. For instance, in current ED2 product a dual-polarized dielectric rod for 28 GHz band operation with cross-polarization ratio greater than 30 dB is used.

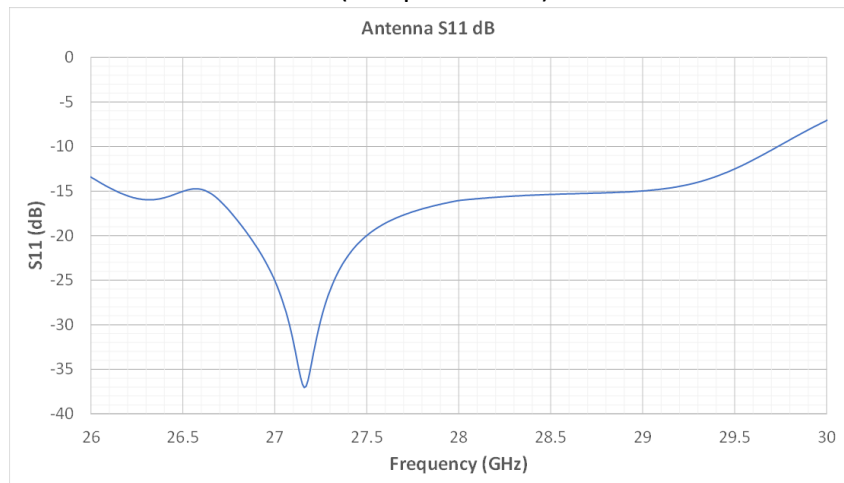


Figure 11: Reflection coefficient of an ED2-dielectric rod, optimized for the n257 5G NR band.

In the case of multiple rods, a switching functionality can be used to electronically activate/deactivate any subset of rods at high speeds (100's of nanoseconds) and dynamically

configure them for transmission or reception. Similarly, for a 5G mmWave repeater that supports TDD (time-division duplexing), switching between the uplink (UL) and downlink (DL) chains of the DU and SU with dielectric antennas can be done in less than 500 nsec, which is well within the TDD switching requirement for 5G operation.

### **Concluding Remarks**

The opening up of millimeter-wave bands for 5G and Beyond communications created new challenges related to the harsh RF propagation environment, but at the same time opened the door for innovations in directional antennas that can largely compensate for channel losses and signal attenuation. Electronically steerable antenna arrays have been a popular choice for analog beamforming in 5G systems, due to the ease of integrating them with RFICs and their earlier deployment at lower frequencies. They are particularly suited for very narrow beamwidth applications under high mobility. However, for use cases involving moderately narrow beamwidths (e.g., 20° nominal HPBW) and pedestrian speeds, or fixed wireless applications (FWA), such flexibility in beam steering becomes an overkill, especially when considering the associated cost, complexity (tens to hundreds of antennas and phase shifters), high power consumption, antenna pattern/gain inconsistency, etc. For 5G repeater applications, a less costly alternative is provided by using dielectric waveguides (rods). A single, inexpensive rod can substitute for an electronically steerable array made from 10s or even 100s of elements; yet the rod exhibits high gain (~ 20 dBi) and a sufficiently narrow beamwidth. Dielectric rods enjoy symmetric patterns and can be mono- or dual-polarized with excellent cross-polarization isolation. They do not require phase shifters, resulting in low production cost. Their wide bandwidth (up to several GHz) makes them ideal for 5G NR repeaters operating at mmWave bands.

### **Author: Marwan M. Krunz**

ED2 Chief Scientist representing partner Wilson Electronics  
Regents Professor, University of Arizona, Electrical and Computer Engineering & Computer Science

Established an NSF Industry/University Cooperative Research Center addressing fundamental research challenges and developing novel technologies for next-generation (5G and beyond) wireless systems through collaborative projects involving academia, industry, and government labs. Dr.Krunz has been dedicated to advancing technology in the areas of 5G systems, shared and dynamic spectrum access, millimeter-wave communications, IoT/sensor systems, wireless cybersecurity, full-duplex communications, MIMO, cognitive radar , mobile edge computing, and others.